Comparison of Simultaneous VGOS and Legacy VLBI Sessions

Matthias Glomsda[1], Manuela Seitz[1], Detlef Angermann[1]

Abstract The VLBI Global Observing System (VGOS) represents the next-generation VLBI system, which consists of a growing network of small and fast-slewing radio antennas performing broadband observations. It has been developed to increase the accuracy and precision of VLBI measurements and the geodetic parameters that can be obtained from analyzing the latter. Ultimately, VGOS is expected to approach the accuracy goals of the Global Geodetic Observing System (GGOS) of the International Association of Geodesy (IAG), which are 1 mm for a terrestrial reference frame (TRF) and 1 mm/decade for its long-term stability. Next to the enlarged bandwidth, these goals shall be achieved by the greater number of observations per unit time with VGOS and the resulting higher temporal resolution for the tropospheric parameters. After first experimental VGOS observations in 2014 and initial global measurement efforts during the Continuous VLBI Campaign in 2017 (CONT17), an operational series of bi-weekly VGOS sessions (denoted by 'VG') has become available in the meantime. Starting in early 2019, this series now has a length of about three years, and the current number of sessions is about twice as large as the number of sessions used for the ITRS 2020 realization. Furthermore, the 'VG' sessions have been scheduled to accompany the legacy VLBI rapid turnaround sessions. Hence, these data provide the opportunity to juxtapose the results of the new VGOS broadband to the legacy S/X-band observations, even though the VGOS antenna networks are rather small and still suffer from an unsatisfactory global distribution. In this presentation, we will compare the parameters (i.e., station coordinates, Earth Orientation Parameters, and radio source positions) that we computed with our DGFI Orbit and Geodetic parameter estimation Software (DOGS) for all available 'VG' sessions between 2019 and 2021 to their respective counterparts in the rapid turnaround sessions. In particular, we will investigate the implied local ties between co-located VGOS and legacy antennas, as well as potential systematic offsets in radio source positions observed at the different frequencies. This might provide valuable information on how to combine the new VGOS with the legacy S/X network.

1. Deutsches Geodätisches Forschungsinstitut der Technischen Universität München

Keywords VGOS, VLBI analysis, EOP

1 Introduction

The next generation of Very Long Baseline Interferometry (VLBI) is represented by the VLBI Global Observing System (VGOS; Petrachenko et al., 2009). By the end of 2021, it consisted of nine operational radio antennas, which simultaneously observe four bands in a frequency range between 3 and 11 GHz instead of the distinct legacy S (about 2 GHz) and X (about 8 GHz) bands. These VGOS antennas are usually smaller, stiffer, and faster-slewing than the legacy antennas. This makes them less sensitive to gravitational deformation, and it allows for more observations per unit time. With the latter, a higher resolution of parameters describing the atmospheric refraction of the radio signal becomes possible. Furthermore, the VLBI observable, i.e., the signal delay between each of the two antennas forming a baseline,

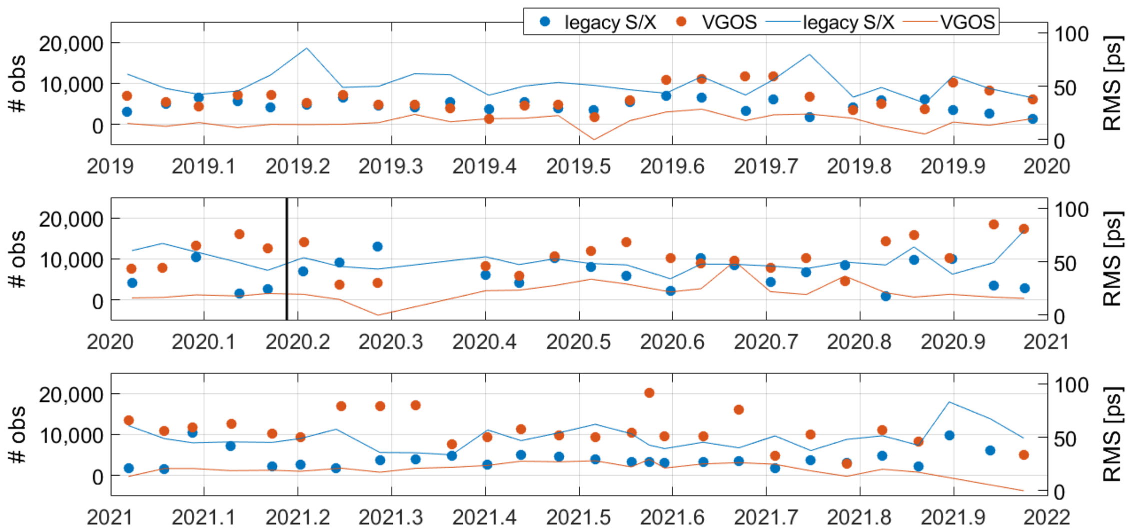

Fig. 1 Number of observations (dots, left Y-axis) and RMS of post-fit residuals (lines, right Y-axis) for both legacy S/X (blue) and simultaneous VGOS (red) sessions between 2019 and 2021. The black vertical line represents the approximate barrier between sessions used (before) and not used (after) for the ITRF2020.

is supposed to be more accurate and more precise with VGOS.

The history of VGOS observations is rather short yet. However, between 2019 and 2021, about 75 VGOS sessions have been performed and correlated (i.e., twice a month), which finally enables the analysis of a firm set of data. For comparison, these sessions have each been scheduled to overlap with a legacy rapid turnaround session. The starting epochs of both the VGOS and the simultaneous legacy sessions are shown on the X-axis of Figure 1. On the left Y-axis, the number of observations per session is depicted. The right Y-axis represents the root mean square (RMS) error of the observation residuals in a least-squares fit of geodetic parameters to these observations (compare below). From the figure, one can see that, for the VGOS sessions, the number of observations is generally larger, although the number of participating stations per session is at most nine for VGOS, while there are about 10–12 stations involved in the legacy rapid turnaround sessions. As mentioned before, this is a result of the faster-slewing VGOS antennas. Since the latter also provide more precise observations, the RMS of post-fit residuals is generally smaller (average across sessions: 18.8 ps) than for the legacy observations (50.3 ps).

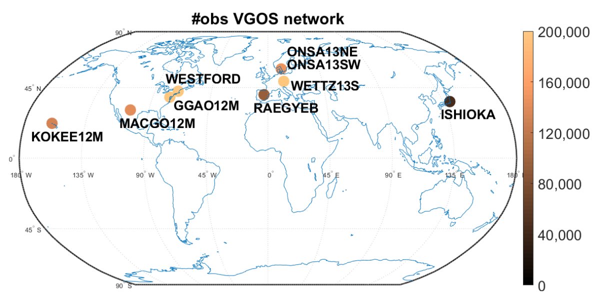

Fig. 2 The operational VGOS station network at the end of 2021. The color code indicates the number of observations per station across all sessions between 2019 and 2021.

The operational VGOS station network as of December 2021 is shown in Figure 2. It is restricted to the Northern hemisphere.

2 Analysis Setup

To compare their geodetic results, we analyzed the simultaneous VGOS and legacy S/X sessions with our DGFI Orbit and Geodetic parameter estimation Software (DOGS; Gerstl et al., 2000). For each session, we estimated constant station positions at midnight, the full set of Earth orientation parameters (EOP, terrestrial pole offsets and drifts, UT1-UTC and LOD, and celestial pole offsets) at the session's mid epoch, and constant radio source coordinates at epoch 2015.0 (the reference epoch of the Third International Celestial Reference Frame, ICRF3; Charlot et al., 2020). As auxiliary parameters, we also included piece-wise linear tropospheric zenith and gradient delays, as well as clock correction terms (quadratic plus piece-wise linear offsets). The corresponding observation and normal equations were set up with DOGS-RI (Radio Interferometry), while we added the datum constraints and inverted the final normal matrix with DOGS-CS (Combination & Solution).

The geophysical models used are basically the same as those applied in our DGFI-TUM Analysis Center solution 'dgf2020a' for the International VLBI Service for Geodesy and Astrometry (IVS). For the VGOS sessions, however, we increased the resolution for the tropospheric zenith (1h to 0.25h) and gradient delays (6h to 1h) to exploit the larger number of observations per unit time. Although the VGOS observations refer to broadband, and radio source positions potentially change with frequency (e.g., Petrachenko et al., 2009), we had to apply the same a priori source coordinates as for the legacy observations (ICRF3 S/X), because there is no broadband frame yet.

The major difference w.r.t. 'dgf2020a' is the a priori station positions. Because the previous International Terrestrial Reference Frame (ITRF2014; Altamimi et al., 2016) does not contain the coordinates of the VGOS stations, we used a preliminary realization of the International Terrestrial Reference System (ITRS) 2020 for VLBI stations that we computed at DGFI-TUM. It will be called 'DTRF2020VP' in the following, and it is based on the official IVS input to the ITRS 2020 realization (Hellmers et al., 2021). DTRF2020VP combines the VGOS and legacy networks by EOP, local ties, mixed-mode sessions, ONTIE sessions (Varenius et al., 2021), three antennas that participated in both networks (ISHIOKA, RAEGYEB, and WESTFORD), and the velocities of co-located VGOS and legacy antennas.

Finally, the geodetic datum was constrained as follows: there are a no-net-rotation (NNR) condition w.r.t. the defining sources of ICRF3 S/X, as well as both no-net-translation (NNT) and NNR conditions w.r.t. stable stations in DTRF2020VP. In particular, the VGOS stations ISHIOKA, MACGO12M, and WETTZ13S are not among the datum stations, as they had large transformation residuals.

3 Comparison of Geodetic Parameters

3.1 EOP w.r.t. IERS 14 C04

The common benchmark for estimated EOP is the 14 C04 series (Bizouard et al., 2019) of the International Earth Rotation and Reference Systems Service (IERS). We interpolated the estimated EOP from the simultaneous VGOS and legacy sessions to common epochs and computed the differences w.r.t. the C04 series for each observation mode. Table 1 lists the weighted means as well as the weighted root-mean-square (WRMS) values of these differences.

Table 1 Statistics of the differences between the IERS 14 C04 series and the EOP estimated for the simultaneous VGOS and legacy sessions between 2019 and 2021.

EOP	unit	wmean legacy	wmean VGOS	WRMS legacy	WRMS VGOS
x-pol	[µas]	−3.2	−192.9	107.4	266.1
x-pol rate	[µas/d]	18.3	9.0	215.1	297.8
y-pol	[µas]	−36.8	−112.4	115.5	255.7
y-pol rate	[µas/d]	−14.7	116.3	222.7	285.0
UT1-UTC	[µs]	9.0	5.1	10.9	13.8
LOD	[µs/d]	2.1	6.4	16.2	14.6
DXCIP	[µas]	−8.7	−1.7	109.7	454.1
DYCIP	[µas]	−9.1	104.2	109.6	443.9

We obtain significant offsets between C04 and the VGOS EOP for polar motion (except for the x-pol rate) and the Y component of the celestial pole offsets. The size of these offsets depends on the choice of VGOS datum stations, i.e., it changes if all VGOS stations are used for the NNT and NNR conditions (not shown here). Possible reasons are the Northern hemisphere bias of the VGOS station network or residual rotations between the VGOS and legacy networks in our a priori TRF, DTRF2020VP. The WRMS values for the terrestrial and celestial pole parameters are also significantly larger for the VGOS sessions. For UT1-UTC and its reverse-signed rate (length-of-day, LOD) on the other hand, there are neither offsets nor increased WRMS values, which is in line with the East-West distribution of VGOS baselines.

3.2 Formal Errors

Because the measurement precision of VGOS is better than for the legacy S/X observations, one would expect the formal errors of the estimated parameters to decrease for the VGOS sessions. While this is the case for the station coordinates (see Figure 3), we could not confirm this for the EOP or the source coordinates yet. This may again be related to the imperfect VGOS station distribution.

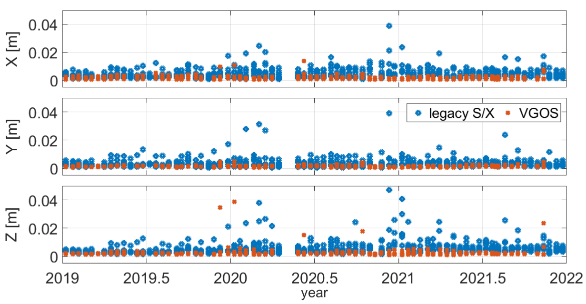

Fig. 3 Formal errors (Y-axis) for all station coordinates in the simultaneous VGOS (red) and legacy (blue) sessions. The X-axis refers to the parameter epoch, which is the same for all coordinates within the same session.

3.3 Co-location Velocities

There are four sites with co-located VGOS and legacy antennas: Kokee Park, Hawaii; Onsala, Sweden (with two VGOS antennas); Wettzell, Germany; and Yebes, Spain. In the DTRF2020VP, the a priori velocities of the co-located antennas are basically equal, because they have been constrained accordingly. However, if we estimate the velocities from the a posteriori positions for each distinct antenna, we sometimes obtain quite different velocities for the co-located VGOS and legacy antennas. For example, Figure 4 shows the X-coordinates of the co-located stations KOKEE12M (VGOS) and KOKEE (legacy S/X). In this case, the fitted a posteriori velocities differ by almost 7 mm/yr.

Generally, a discrepancy can be expected, because the used time series are rather short (three years), and there are different numbers of sessions related to the VGOS and the legacy antennas. For KOKEE12M, however, there is another effect: there is a bunch of

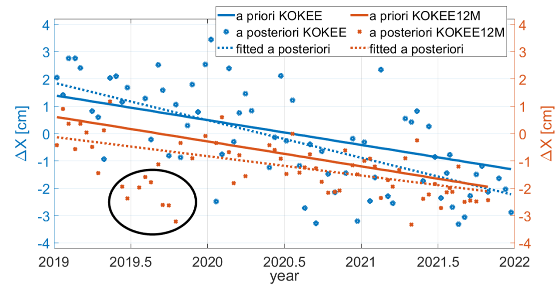

Fig. 4 A priori and estimated x-coordinates of the co-located antennas KOKEE (legacy, blue, $-5,543,837.84$ m + ΔX) and KOKEE12M (VGOS, red, $-5,543,831.75$ m + ΔX) at Kokee Park. In the VGOS sessions within the black ellipse, ISHIOKA was not part of the VGOS network.

VGOS sessions (indicated by the black ellipse) with quite different a posteriori coordinates compared to the other ones. In these sessions, ISHIOKA was not part of the VGOS station network. From Figure 2, we learn that the network volume is much smaller without the remote station ISHIOKA, and the sky coverage at KOKEE12M is much worse, too. If we exclude these inferior sessions from the velocity fit, the fitted value for KOKEE12M's x-coordinate only differs by 0.13 mm/yr from its (DTRF2020VP) a priori value.

3.4 Local Ties

We computed 'cross-session local ties' for all epochs t with both a VGOS and a legacy S/X session containing a co-location site, and we compared them to the official local ties LT_i:

$$\left[S_i^{VGOS}(t) - S_i^{legacy}(t)\right] - LT_i \,, \qquad (1)$$

with S_i $(i = x,y,z)$ representing the estimated station coordinates per session. This measure is quite noisy, because we compute the differences between two random variables. However, systematic differences might indicate discrepancies between the co-located antennas or problems with the official local ties. In Figure 5, the cross-session local ties of Equation (1) have been transformed to the local North, East, and Up coordinate system, and we actually observe some systematic behavior: the cross-session local ties are almost exclusively larger than the official local ties for both the Up direction at Yebes and the East direction at Kokee Park.

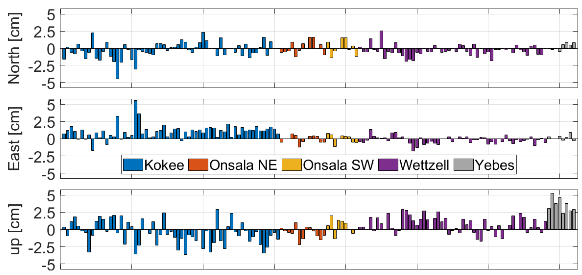

Fig. 5 The 'cross-session local ties' of Equation (1) at the co-location sites rotated from the Cartesian to the local coordinate system.

For Wettzell, the distribution of these ties does not look completely random, either.

4 Source Coordinates

VGOS measurements cover a broader frequency range than the legacy S/X observations. Because source positions are frequency and time dependent, we might expect to estimate systematically different source coordinates from the two observation modes. There are 203 sources which have been observed in both VGOS and legacy S/X sessions. Out of these, 58 are contained in at least 20 sessions for both modes. We fitted constant coordinates at epoch 2015.0 to the estimated source coordinates of the VGOS and legacy S/X sessions, respectively. Figure 6 shows that the fitted coordinates actually deviate, but the differences are generally smaller than the scatter of the estimated coordinates itself (which is generally larger for VGOS, especially for negative declinations due to missing Southern hemisphere stations). Hence, we are not able to distinguish VGOS and legacy S/X source positions yet.

5 Conclusion

The geodetic parameters estimated from VGOS observations are already promising. However, there still are discrepancies w.r.t. the legacy S/X observations, which might mainly be attributable to the inferior station distribution of the VGOS network. Hence, the expected improvements in terms of accuracy and precision are not fully realized yet.

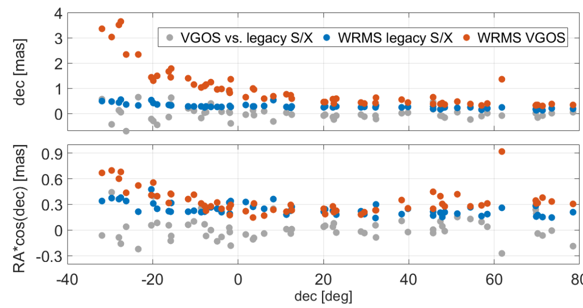

Fig. 6 The differences (grey) between the constant declinations (top) and right ascensions (bottom) as fitted for each common source (X-axis) from VGOS and legacy S/X sessions. For comparison, also the WRMS values for both VGOS (red) and legacy (blue) sessions are given, representing the scatter of estimated source coordinates around their fitted coordinate.

References

Altamimi Z., Rebischung P., Metivier L., and Collilieux X. (2016): ITRF2014: A new release of the International Terrestrial Reference Frame modeling nonlinear station motions. *J. Geophys. Res. Solid Earth*, Vol. 121 (8), pp. 6109-6131.

Bizouard C., Lambert S., Gattano C., Becker O., and Richard J.Y. (2019): The IERS EOP 14C04 solution for Earth orientation parameters consistent with ITRF 2014. *J. Geod.*, Vol. 93, pp. 621-633.

Charlot P., Jacobs C.S., et al. (2020): The third realization of the International Celestial Reference Frame by very long baseline interferometry. *A&A*, 644.

Gerstl M., Kelm R., Müller H., and Ehrnsperger W. (2000): DOGS-CS – Kombination und Lösung großer Gleichungssysteme. *Int. Rep.*, DGFI-TUM.

Hellmers H., Modiri S., Bachmann S., Thaller D., Bloßfeld M., Seitz M., Gipson J. (2021): Combined IVS contribution to the ITRF2020. *Proceedings of the 25th EVGA Working Meeting*, pp. 61–65.

Petrachenko B., Niell A., et al. (2009): Design aspects of the VLBI2010 system. Progress report of the VLBI2010 committee. *NASA/TM-2009-214180*.

Varenius E., Haas R., and Nilsson T. (2021): Short-baseline interferometry local-tie experiments at the Onsala Space Observatory. *J. Geod.*, Vol. 95 (54).